# Offset-QAM based coherent WDM for spectral efficiency enhancement

**J. Zhao* and A. D. Ellis**

*Photonic Systems Group, Tyndall National Institute and Department of Physics, University College Cork, Lee Maltings, Prospect Row, Cork, Ireland*
**jian.zhao@tyndall.ie*

**Abstract:** Optically multiplexed multi-carrier systems with channel spacing reduced to the symbol rate per carrier are highly susceptible to inter-channel crosstalk, which places stringent requirements for the specifications of system components and hinders the use of high-level formats. In this paper, we investigate the performance benefits of using offset 4-, 16-, and 64-quadrature amplitude modulation (QAM) in coherent wavelength division multiplexing (CoWDM). We compare this system with recently reported Nyquist WDM and no-guard-interval optical coherent orthogonal frequency division multiplexing, and show that the presented system greatly relaxes the requirements for device specifications and enhances the spectral efficiency by enabling the use of high-level QAM. The achieved performance can approach the theoretical limits using practical components.



**OCIS codes:** (060.2330) Fiber optics communications; (060.4080) Modulation.

## References and links

1. X. Zhou, J. Yu, M. F. Huang, Y. Shao, T. Wang, L. Nelson, P. Magill, M. Birk, P. I. Borel, D. W. Peckham, and R. Lingle, "64Tb/s (640×107Gb/s) PDM-36QAM transmission over 320km using both pre- and post-transmission digital equalization," *Optical Fiber Communication Conference* (2010), paper PDPB9.
2. A. Sano, E. Yamada, H. Masuda, E. Yamazaki, T. Kobayashi, E. Yoshida, Y. Miyamoto, R. Kudo, K. Ishihara, and Y. Takatori, "No-guard-interval coherent optical OFDM for 100Gb/s long-haul WDM transmission," J. Lightwave Technol. **27**(16), 3705–3713 (2009).
3. S. Chandrasekhar and X. Liu, "Experimental investigation on the performance of closely spaced multi-carrier PDM-QPSK with digital coherent detection," Opt. Express **17**(24), 21350–21361 (2009).
4. J. Yu, Z. Dong, X. Xiao, Y. Xia, S. Shi, C. Ge, W. Zhou, N. Chi, and Y. Shao, "Generation, transmission and coherent detection of 11.2 Tb/s (112×100Gb/s) single source optical OFDM superchannel," *Optical Fiber Communication Conference* (2011), paper PDPA6.
5. G. Bosco, A. Carena, V. Curri, P. Poggiolini, and F. Forghieri, "Performance limits of Nyquist-WDM and Co-OFDM in high-speed PM-QPSK systems," IEEE Photon. Technol. Lett. **22**(15), 1129–1131 (2010).
6. A. D. Ellis and F. C. G. Gunning, "Spectral density enhancement using coherent WDM," IEEE Photon. Technol. Lett. **17**(2), 504–506 (2005).
7. J. Zhao and A. D. Ellis, "A novel optical fast OFDM with reduced channel spacing equal to half of the symbol rate per carrier," *Optical Fiber Communication Conference* (2010), paper OMR1.
8. S. Yamamoto, K. Yonenaga, A. Sahara, F. Inuzuka, and A. Takada, "Achievement of sub-channel frequency spacing less than symbol rate and improvement of dispersion tolerance in optical OFDM transmission," J. Lightwave Technol. **28**(1), 157–163 (2010).
9. Y. Cai, J. X. Cai, C. R. Davidson, D. Foursa, A. Lucero, O. Sinkin, A. Pilipetskii, G. Mohs, and S. N. Bergono, "High spectral efficiency long-haul transmission with pre-filtering and maximum a posteriori probability detection," Proc. *European Conference on Optical Communication* (2010), paper We.7.C.4.
10. R. R. Mosier and R. G. Clabaugh, "Kineplex, a bandwidth-efficient binary transmission system," AIEE Trans. Commun. **76**, 723–728 (1958).
11. R. W. Chang, "Synthesis of band-limited orthogonal signals fro multi-channel data transmission," Bell Syst. Tech. J. **45**, 1775–1796 (1966).
12. S. B. Weinstein and P. M. Ebert, "Data transmission by frequency division multiplexing using the discrete Fourier transform," IEEE Trans. Commun. Technol. Com. **19**(5), 628–634 (1971).
13. J. Zhao and A. D. Ellis, "Electronic impairment mitigation in optically multiplexed multi-carrier systems," J. Lightwave Technol. **29**(3), 278–290 (2011).
14. G. Gavioli, E. Torrengo, G. Bosco, A. Carena, V. Curri, V. Miot, P. Poggiolini, M. Belmonte, F. Forghieri, C. Muzio, S. Piciaccia, A. Brinciotti, A. L. Porta, C. Lezzi, S. Savory, and S. Abrate, "Investigation of the impact of

#148015 - $15.00 USD Received 25 May 2011; revised 7 Jul 2011; accepted 8 Jul 2011; published 14 Jul 2011

ultra-narrow carrier spacing on the transmission of a 10-carrier 1Tb/s superchannel," *Optical Fiber Communication Conference* (2010), paper OThD3.
15. D. Hillerkuss, T. Schellinger, R. Schmogrow, M. Winter, T. Vallaitis, R. Bonk, A. Marculescu, J. Li, M. Dreschmann, J. Meyer, S. Ben Ezra, N. Narkiss, B. Nebendahl, F. Parmigiani, P. Petropoulos, B. Resan, K. Weingarten, T. Ellermeyer, J. Lutz, M. Moller, M. Huebner, J. Becher, C. Koos, W. Freude, and J. Leuthold, "Single source optical OFDM transmitter and optical FFT receiver demonstrated at line rates of 5.4 and 10.8 Tbit/s," *Optical Fiber Communication Conference* (2010), paper PDPC1.
16. S. K. Ibrahim, J. Zhao, F. C. Garcia Gunning, P. Frascella, F. H. Peters, and A. D. Ellis, "Coherent WDM: analytical, numerical, and experimental studies," IEEE Photon. J. **2**(5), 833–847 (2010).
17. J. G. Proakis, *Digital Communications*, 4th ed. (McGraw-Hill, 2000).
18. B. Hirosaki, S. Hasegawa, and A. Sabato, "Advanced groupband data modem using orthogonally multiplexed QAM technique," IEEE Trans. Commun. **34**(6), 587–592 (1986).

## 1. Introduction

The rapid growth in video based Internet applications is increasing the demand for spectrally-efficient optical communication systems. Spectral efficiency can be increased by either using higher-level modulation formats or reducing the channel spacing. In conventional wavelength division multiplexing (WDM) systems, a channel spacing equal to 1.2 times symbol rate per carrier using 36-quadrature amplitude modulation (QAM) was reported [1]. According to communication theory, it is possible to reduce the channel spacing to the symbol rate per carrier without any penalty from inter-channel crosstalk or intersymbol interference (ISI). For ultra-high-speed optical communications, this concept has been implemented by using optically multiplexed multi-carrier systems, including no-guard-interval coherent orthogonal frequency division multiplexing (OFDM) [2–4], Nyquist wavelength division multiplexing (N-WDM) [5], and coherent WDM (CoWDM) [6]. When the channel spacing is further reduced, crosstalk and/or ISI free operation cannot be achieved unless single-quadrature format is used [7], or the channel number $J$ is small (e.g. $J = 2$) and the occupied bandwidth is $\sim(J + 1)/T$, where $T$ is the symbol period, resulting in redundancy in the spectral usage [8]. In [9], a pre-filtered 28Gsym/s 4-QAM system with 25GHz channel spacing was reported, which employed maximum a posteriori probability detection to mitigate the inevitable ISI.

In optically multiplexed multi-carrier systems with channel spacing equal to the symbol rate per carrier, it is essential to ensure orthogonality between channels so that they can be demultiplexed at the receiver without inter-channel crosstalk. Here, orthogonality [10,11] is a broad term and is not limited to the use of rectangular waveform (or sinc-function based spectral profile) as in discrete-Fourier-transform (DFT) based OFDM [12]. In fact, due to a high symbol rate per carrier (~10-40Gsym/s) in optically multiplexed multi-carrier systems, rectangular pulses with infinite spectral tails cannot be obtained by any practical devices, which commonly have bandwidths less than 50GHz. Consequently, ideal orthogonality cannot be achieved. In the no-guard-interval coherent optical OFDM system employing more than two channels, this residual crosstalk limits the achievable format level to 4-QAM even when a stringently specified digital signal processing (DSP) based receiver filter is employed [3]. To improve the receiver sensitivity and relax the requirements of the receiver-side filter, a bandwidth limited solution, N-WDM, has been proposed, in which an extra optical filter is used for pre-filtering [5]. However, N-WDM aims for a rectangular spectral profile (or sinc-function based pulse shape), which is still difficult to achieve. Consequently, residual inter-channel crosstalk also exists even with careful design of the optical [5] or DSP-based [13] pre-filter. This residual crosstalk, as will be shown in this paper, not only increases the difficulty of the filter design at the transmitter and the required memory length of the receiver digital filter, but also hinders the use of 16- and 64-QAM. Note that an extra guard band (or interval) can be used to alleviate the impact of the crosstalk in N-WDM (or OFDM) [14,15]. However, systems with additional guard band only offer the same information spectral density as conventional dense WDM and will not be considered in this paper.

CoWDM [6] is one class of optically multiplexed multi-carrier systems with channel spacing equal to the symbol rate per carrier, which is distinguished by the use of extra phase

#148015 - $15.00 USD Received 25 May 2011; revised 7 Jul 2011; accepted 8 Jul 2011; published 14 Jul 2011

control at the transmitter to mitigate the inter-channel crosstalk. However, conventional CoWDM only uses single-quadrature formats, e.g. on-off keying [6] or binary phase shifted keying [16], and it has been shown that the phase control cannot be used to mitigate the crosstalk with two-quadrature formats [13]. In this paper, we propose a CoWDM system using offset 4-, 16-, and 64-QAM. Offset QAM is a group of modulation formats in general communications [17], and has been implemented using the DFT technique for data modems [18]. We derive the conditions for crosstalk and ISI free operation in offset-QAM CoWDM and find that the use of this group of formats can significantly relax the requirements for optimum operation of CoWDM. By offsetting the in-phase and quadrature tributaries by half symbol period in time, the crosstalk and ISI can be eliminated even using practical signal spectral profile or pulse shape. We compare this system with N-WDM and no-guard-interval optical OFDM, and show that the presented system significantly improves the performance and consequently enhances the spectral efficiency by enabling the use of high-order offset QAM, with the performance approaching the theoretical limits using practical components.

The paper is organized as follows. In Section 2, we describe the principle of offset-QAM CoWDM, including the theoretical derivations to obtain the conditions for crosstalk and ISI free operation and semi-analytical analysis on crosstalk levels to illustrate its performance benefits. Based on the implications of the analysis, Section 3 gives the simulation setup and Section 4 shows that the presented system significantly improves the performance and relaxes the system specifications. Finally, Section 5 summarizes the results.

## 2. Principle

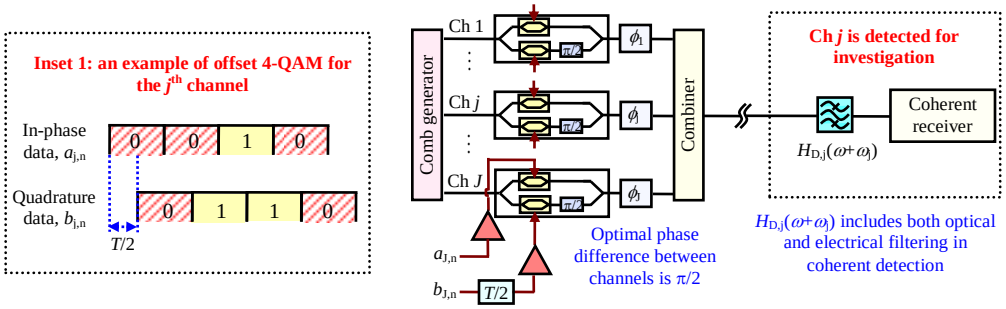


Fig. 1. The model of offset-QAM CoWDM for theoretical analysis. Inset 1: the offset 4-QAM data for modulation.

The principle of single-carrier offset QAM has been described in general communications [17]. As shown in the Inset 1 of Fig. 1, the quadrature signal is delayed by $T/2$ with respect to the in-phase signal before modulation at the transmitter, where $T$ is the symbol period. In the single-channel case, the use of offset QAM would eliminate the amplitude fluctuations associated with π phase shift. In this paper, we will focus on how the use of this group of formats would relax the required condition to approach crosstalk free operation in CoWDM with two-quadrature formats and consequently improve the performance. Figure 1 depicts the model of analysis. We define $E_j(t)$ as the optical field of the signal after the demultiplexing filter targeted to demultiplex the $j^{th}$ channel. Here, $E_j(t)$ is the baseband representation:

$$E_j(t) = E_0 \sum_{k=1}^{J} \sum_{n=-\infty}^{\infty} (a_{k,n} I_{k,j}(t-nT) + i \cdot b_{k,n} Q_{k,j}(t-nT)) e^{i(\omega_k - \omega_j)\cdot nT + i\phi_k} \qquad (1)$$

where $E_0$ and $J$ are a constant and the number of channels respectively. $a_{k,n}$ and $b_{k,n}$ are the $n^{th}$ logic data of the in-phase and quadrature tributaries of the $k^{th}$ channel respectively. $\omega_k$ and $\phi_k$ are the frequency and phase of the $k^{th}$ carrier respectively. $I_{k,j}(t)$ and $Q_{k,j}(t)$ are the signal pulses of the in-phase and quadrature tributaries of the $k^{th}$ channel after the filter targeted to

#148015 - $15.00 USD Received 25 May 2011; revised 7 Jul 2011; accepted 8 Jul 2011; published 14 Jul 2011

demultiplex the $j^{th}$ channel, and represent the overall impulse response of the whole system. $I_{k,j}(t)$ and $Q_{k,j}(t)$ are related to the baseband pulse shape of the signal before demultiplexing, $h_s(t)$, and the impulse response of the demultiplexing filter for the $j^{th}$ channel, $h_{D,j}(t)$, by:

$$I_{k,j}(t) = \int_{-\infty}^{+\infty} h_s(t-\tau) e^{i(\omega_k-\omega_j)(t-\tau)} \cdot h_{D,j}(\tau) e^{-i\omega_j\tau} d\tau \tag{2.1}$$

$$Q_{k,j}(t) = \int_{-\infty}^{+\infty} h_s(t-\tau-T/2) e^{i(\omega_k-\omega_j)(t-\tau)} \cdot h_{D,j}(\tau) e^{-i\omega_j\tau} d\tau \tag{2.2}$$

We define $H_{\text{in-phase,k,j}}(\omega)$, $H_{\text{quadrature,k,j}}(\omega)$, $H_s(\omega)$, $H_{D,j}(\omega)$ as the Fourier transforms of $I_{k,j}(t)$, $Q_{k,j}(t)$, $h_s(t)$, $h_{D,j}(t)$ respectively, and have:

$$H_{in-phase,k,j}(\omega) = H_s(\omega-\omega_k+\omega_j) \cdot H_{D,j}(\omega+\omega_j) \tag{3.1}$$

$$H_{quadrature,k,j}(\omega) = H_s(\omega-\omega_k+\omega_j) \cdot e^{-i(\omega-\omega_k+\omega_j)T/2} H_{D,j}(\omega+\omega_j) \tag{3.2}$$

Here $H_s(\omega)$ represents the overall baseband system response before demultiplexing, including the transmitted electrical signal pulse shape, the transfer functions of the driving amplifier and the modulator, chromatic dispersion in the fiber link etc. $H_{D,j}(\omega + \omega_j)$ here represents the receiver-side filter for channel demultiplexing, and, in coherent detection, should include both the optical filtering, $H_{opt,j}(\omega + \omega_j)$, and the electrical filtering, $H_{ele,j}(\omega + \omega_j\text{-}\omega_{lo})$:

$$H_{D,j}(\omega+\omega_j) = H_{opt,j}(\omega+\omega_j) \cdot H_{ele,j}(\omega+\omega_j-\omega_{lo}) \tag{4}$$

where $\omega_{lo}$ is the frequency of the local oscillator. In practice, $H_{D,j}(\omega + \omega_j)$ is usually matched to $H_s(\omega)$, i.e. $H_{D,j}(\omega + \omega_j) = H_s^*(\omega)$, to minimize the noise impact, which is achieved by using digital filters at the receiver. Therefore, the number of free parameters is reduced and the problem degenerates to the design of only $H_s(\omega)$ to achieve crosstalk and ISI free operation.

Due to the close channel spacing, the demultiplexing filter for the channel $j$, $H_{D,j}(\omega + \omega_j)$, may allow through parts of the signals from other channels, e.g. channels ($j$-1) and ($j$ + 1), in addition to the targeted channel, such that $I_{k,j}(t)$ and $Q_{k,j}(t)$ ($k \neq j$) are not zero for all $t$. However, the symbol decisions are made based only on the final samples of the signal, where the final decision samples are those obtained after all over- or non-over-sampling based digital processing in coherent detection. Consequently, we only require that the crosstalk and ISI levels at the final sampling points are zero. By setting $t = mT$ and $(m + 0.5)T$ in Eq. (1) for the in-phase and quadrature tributaries respectively, we have the decoded logical data $a'_{j,m}$ and $b'_{j,m}$:

$$\begin{aligned} a'_{j,m} \propto real\{&(a_{j,m}I_{j,j}(0) + i\cdot b_{j,m}Q_{j,j}(0)) + \sum_{n\neq m}(a_{j,n}I_{j,j}((m-n)T) + i\cdot b_{j,n}Q_{j,j}((m-n)T)) \\ &+ \sum_{k\neq j}\sum_{n}(a_{k,n}I_{k,j}((m-n)T) + i\cdot b_{k,n}Q_{k,j}((m-n)T))e^{i(\phi_k-\phi_j)}\} \end{aligned} \tag{5.1}$$

$$\begin{aligned} b'_{j,m} \propto imag\{&(a_{j,m}I_{j,j}(0.5T) + i\cdot b_{j,m}Q_{j,j}(0.5T)) + \sum_{n\neq m}(a_{j,n}I_{j,j}((m-n+0.5)T) + i\cdot b_{j,n}Q_{j,j}((m-n+0.5)T)) \\ &+ \sum_{k\neq j}\sum_{n}(a_{k,n}I_{k,j}((m-n+0.5)T) + i\cdot b_{k,n}Q_{k,j}((m-n+0.5)T))e^{i(\phi_k-\phi_j)}\} \end{aligned} \tag{5.2}$$

Here we use the property of $(\omega_k\text{-}\omega_j) = 2\pi(k\text{-}j)/T$. The first, second, and third terms on the right-hand of Eqs. (5.1) and (5.2) represent the signal, ISI, and crosstalk, respectively. Note that in Eq. (5), the phase of the targeted $j^{th}$ channel, $\phi_j$, is assumed to be compensated. In practice, similar to other coherent-detection systems, $\phi_j$ varies with time and an adaptive algorithm is

#148015 - $15.00 USD Received 25 May 2011; revised 7 Jul 2011; accepted 8 Jul 2011; published 14 Jul 2011

required to mitigate the impact of phase noise, unless the laser linewidth is sufficiently narrow and $\phi_j$ is approximately constant for the acquired data window.

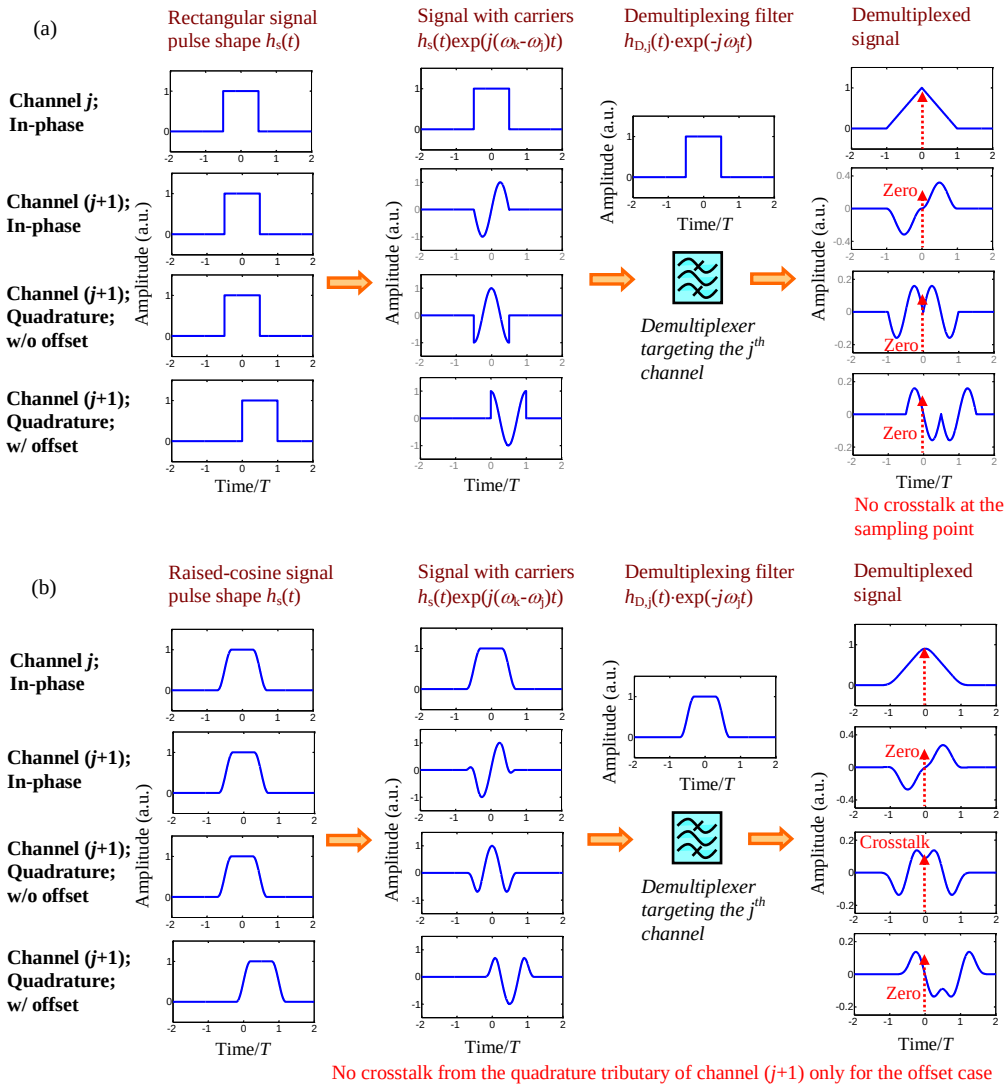


Fig. 2. An example to illustrate the crosstalk from the in-phase and quadrature tributaries of the $(j + 1)^{th}$ channel to the in-phase tributary of the $j^{th}$ channel by using a signal pulse of (a) rectangular and (b) raised cosine with the roll-off coefficient of 0.4. The first, second, and fourth columns show the signals before demultiplexing without and with normalized carriers with respect to the $j^{th}$ channel, and after demultiplexing respectively, when the input signal is the in-phase tributary of the $j^{th}$ (the top row) and $(j + 1)^{th}$ (the second row) channels, and the quadrature tributary of the $(j + 1)^{th}$ channel without (the third row) and with (the bottom row) $T/2$ time offset. The third column shows the impulse response of the demultiplexing filter for the $j^{th}$ channel. In both figures, $\phi_j = 0$ and $\phi_{j+1} = \pi/2$.

The optimum operation for a general optically multiplexed multi-carrier system requires:

1. Matched filter to minimize the noise impact, which places restrictions on the selection of the receiver filter ($H_{D,j}(\omega + \omega_j) = H_s^*(\omega)$) but not on the transmitted signal pulse shape;

#148015 - $15.00 USD Received 25 May 2011; revised 7 Jul 2011; accepted 8 Jul 2011; published 14 Jul 2011

2. Nyquist ISI criterion for ISI free operation in generic communication systems, which is satisfied by only particular set of signal pulse shapes with associated matched receiver filters. Fortunately, the selection of signal pulse shape under this restriction is not stringent and a signal generated by a practical transmitter in the conventional WDM or single-channel case can achieve ISI free operation, unless the system is bandwidth-limited [1,9];
3. Channel orthogonality specific to optically multiplexed multi-carrier systems for crosstalk free operation. This condition strictly limits the freedom of selecting the spectral profiles of the signal before demultiplexing ($H_s(\omega)$) and the associated matched filter ($H_{D,j}(\omega + \omega_j)$).

As the conditions for the matched filter and ISI free operation of a particular channel are similar to those in the single-channel case, we will assume that these two conditions are satisfied and focus on the analysis of inter-channel crosstalk, i.e. the third term on the right hand of Eqs. (5.1) and (5.2). In conventional optically multiplexed multi-carrier systems, the requirement for channel orthogonality is strict. In recently reported works, rectangular- (no-guard-interval optical OFDM) and sinc-function (N-WDM) based signal pulse shapes have been used. Figure 2(a) illustrates the example using a rectangular signal pulse shape. As depicted in the second and third rows of the figure, the crosstalk from the in-phase and quadrature tributaries of the $(j + 1)^{th}$ channel to the targeted $j^{th}$ channel at the sampling point, equal to the integration of the sine and cosine wave over the time period of $T$, is zero. However, precluded by the limitations of device fabrication, these signal pulses cannot be practically realized. On the other hand, commonly used practical signal pulses do not satisfy the condition for crosstalk free operation or channel orthogonality, as depicted by the second and third rows of Fig. 2(b) where the signal pulse is a raised cosine with roll-off coefficient of 0.4. The figure clearly shows that crosstalk exists. It is also observed that when the carrier phase difference between channels is $\pi/2$, the crosstalk is only from the other quadrature of the $(j + 1)^{th}$ channel. This is the principle of conventional CoWDM [13], where with single-quadrature modulation, crosstalk free operation can be achieved even with practical components.

*2.1 Relaxed Condition for Crosstalk Free Operation*

Figure 2(a) and 2(b) also depict the case when the signal of the quadrature tributary of the $(j + 1)^{th}$ channel is offset by $T/2$ in time (the bottom row). It can be seen that in this specific example, the crosstalk from both the in-phase and quadrature tributaries of the $(j + 1)^{th}$ channel becomes zero even for the practical raised-cosine pulse shape. This implies that potential performance benefits could be obtained by offset-QAM CoWDM. Note that in Fig. 2(b), as will be shown later, crosstalk and ISI free operation is still not ideally achieved because the spectrum of a raised-cosine shaped pulse remains infinite such that the crosstalk from channels ($j$-2) and ($j$ + 2) are not eliminated. In this subsection, we will firstly identify the condition to obtain the optimum operation of offset-QAM CoWDM. For a simple illustration, we firstly study the crosstalk levels to the in-phase tributary of the targeted $j^{th}$ channel (i.e. (5.1)), with $I_{k,j}((m\text{-}n)T)$ and $Q_{k,j}((m\text{-}n)T)$ obtained from Eq. (2):

$$I_{k,j}((m-n)T) = \int_{-\infty}^{+\infty} h_s((m-n)T-\tau)e^{i2\pi(k-j)((m-n)T-\tau)/T} \cdot h_s^*(-\tau)d\tau \qquad (6.1)$$

$$Q_{k,j}((m-n)T) = \int_{-\infty}^{+\infty} h_s((m-n)T-\tau-T/2)e^{i2\pi(k-j)((m-n)T-\tau)/T} \cdot h_s^*(-\tau)d\tau \qquad (6.2)$$

Here, we have used $(\omega_k\text{-}\omega_j) = 2\pi(k\text{-}j)/T$ and the condition of a matched filter with $H_{D,j}(\omega + \omega_j) = H_s^*(\omega)$. Without giving detailed mathematical manipulations, we simplify Eq. (6) as:

#148015 - $15.00 USD Received 25 May 2011; revised 7 Jul 2011; accepted 8 Jul 2011; published 14 Jul 2011

$$I_{k,j}((m-n)T) = (-1)^{(k-j)(m-n)} \int_{-\infty}^{+\infty} h_s((m-n)T/2+\tau')e^{i2\pi(k-j)\tau'/T} \cdot h_s^*(\tau'-(m-n)T/2)d\tau' \quad (7.1)$$

$$Q_{k,j}((m-n)T) = (-1)^{(k-j)(m-n-0.5)} \int_{-\infty}^{+\infty} h_s((m-n-0.5)T/2+\tau')e^{i2\pi(k-j)\tau'/T} \cdot h_s^*(\tau'-(m-n-0.5)T/2)d\tau' \quad (7.2)$$

We place the first requirement on the signal pulse to achieve channel orthogonality: $h_s(t)$ is a even function (real and symmetric). This applies to the majority of practically generated signals. In systems with transmission impairments such as chromatic dispersion, compensation using optical or digital devices is assumed. By using this kind of signal pulse, it can be proved that in (7), $h_s((m\text{-}n)T/2 + \tau')\cdot h_s^*(\tau'\text{-}(m\text{-}n)T/2)$ and $h_s((m\text{-}n\text{-}0.5)T/2 + \tau')\cdot h_s^*(\tau'\text{-}(m\text{-}n\text{-}0.5)T/2)$ are also even functions. Therefore, (7) can be re-written as:

$$I_{k,j}((m-n)T) = (-1)^{(k-j)(m-n)} \int_{-\infty}^{+\infty} h_s((m-n)T/2+\tau')h_s(\tau'-(m-n)T/2)\cos(2\pi(k-j)\tau'/T)d\tau' \quad (8.1)$$

$$Q_{k,j}((m-n)T) = (-1)^{(k-j)(m-n-0.5)} \int_{-\infty}^{+\infty} h_s((m-n-0.5)T/2+\tau')h_s(\tau'-(m-n-0.5)T/2)\cos(2\pi(k-j)\tau'/T)d\tau' \quad (8.2)$$

Physically, Eq. (8) implies that $I_{k,j}((m\text{-}n)T)$ is always real, while $Q_{k,j}((m\text{-}n)T)$ is imaginary for odd $(k\text{-}j)$ and real for even $(k\text{-}j)$. We then place the second requirement: CoWDM with the phase difference between channels of $\pi/2$. Without loss of generality, we define $\phi_k = (k\text{-}1)\cdot\pi/2$, and can obtain from Eq. (5.1):

$$a'_{j,m} \propto a_{j,m}I_{j,j}(0) - \sum_n a_{j-2,n}I_{j-2,j}((m-n)T) - \sum_n a_{j+2,n}I_{j+2,j}((m-n)T)... \quad (9.1)$$

With the same mathematical manipulations, we can also obtain that $Q_{k,j}((m\text{-}n + 0.5)T)$ is always real, while $I_{k,j}((m\text{-}n + 0.5)T)$ is imaginary for odd $(k\text{-}j)$ and real for even $(k\text{-}j)$. Consequently, the detected logical data for the quadrature tributary of the $j^{th}$ channel, $b'_{j,m}$, is:

$$b'_{j,m} \propto b_{j,m}Q_{j,j}(0.5T) - \sum_n b_{j-2,n}Q_{j-2,j}((m-n+0.5)T)) - \sum_n b_{j+2,n}Q_{j+2,j}((m-n+0.5)T))... \quad (9.2)$$

It is clear from Eqs. (9.1) and (9.2) that the crosstalk to a particular quadrature of a particular channel $j$ has only contributions from the same quadrature of channels more than one channel distant from the targeted channel (i.e. channels $(j\text{-}2)$ and $(j + 2)$ and beyond). Therefore, we place the third requirement for crosstalk free operation: the spectral profiles of the signal and its associated matched receiver filter are designed to avoid the spectral overlap between the targeted channel $j$ and channels $(j\text{-}2)$ and $(j + 2)$.

In summary, crosstalk and ISI free operation in offset-QAM CoWDM can be achieved provided that:

a). The spectral profile of the demultiplexing filter is matched to that of the signal.
b). The design of $h_s(t)$ satisfies Nyquist ISI criterion for ISI free operation.
c). $h_s(t)$ is a even function.
d). The transmitter is coherent with optimal phase difference between channels of $\pi/2$.
e). $h_s(t)$ is designed to avoid the spectral overlaps between the targeted channel (e.g. the $j^{th}$ channel) and channels more than one channel distant (e.g. the $(j\text{-}2)^{th}$ and $(j + 2)^{th}$ channels).

Intuitively, as depicted in Fig. 2, the relaxed condition for offset-QAM CoWDM can be understood that when the carrier phase difference between channels is $\pi/2$, the crosstalk to a particular tributary of the targeted channel from the adjacent channels $(j\text{-}1)$ and $(j + 1)$ can only come from the other tributary, which however experiences a zero crossing at the

#148015 - $15.00 USD Received 25 May 2011; revised 7 Jul 2011; accepted 8 Jul 2011; published 14 Jul 2011

sampling point provided that the signal pulse of the other tributary of the adjacent channels ($j$-1) and ($j$ + 1) is the image of the impulse response of the receiver filter about the time point $T$/4.

*2.2 Crosstalk Analysis*

In the previous subsection, we identified the requirements to enable crosstalk and ISI free operation in offset-QAM CoWDM, and consequently obtained guidelines for system design. In this subsection, we theoretically analyze the crosstalk levels for some practical signal pulse shapes to illustrate the benefits of the presented system. For a simple illustration, we only focus on the crosstalk to the in-phase tributary of the targeted channel (i.e. Eq. (5.1)). For comparison, we also analyze the crosstalk levels using conventional systems without the $T$/2 time offset for the quadrature tributary. From Eq. (5.1), it is clear that the essential step for the semi-analytical crosstalk analysis is to obtain $I_{k,j}((m\text{-}n)T)$ and $Q_{k,j}((m\text{-}n)T)$ given the signal pulse shape and the associated matched receiver filter. By using similar mathematical manipulation to [13], we have:

$$FH_{in-phase,k,j}(\omega) = T\{I_{k,j}(0) + I_{k,j}(-T)e^{i\omega T} + I_{k,j}(T)e^{-i\omega T} + I_{k,j}(-2T)e^{2i\omega T} + I_{k,j}(2T)e^{-2i\omega T} + ...\} \quad (10.1)$$

$$FH_{quadrature,k,j}(\omega) = T\{Q_{k,j}(0) + Q_{k,j}(-T)e^{i\omega T} + Q_{k,j}(T)e^{-i\omega T} + Q_{k,j}(-2T)e^{2i\omega T} + Q_{k,j}(2T)e^{-2i\omega T} + ...\} \quad (10.2)$$

where $\omega \in [-\pi/T\ \pi/T]$ and $k \neq j$. The folded spectra of $I_{k,j}(t)$ and $Q_{k,j}(t)$, $FH_{\text{in-phase},k,j}(\omega)$ and $FH_{\text{quadrature, k,j}}(\omega)$, are defined as:

$$FH_{in-phase,k,j(\omega)} = \sum_{p=-\infty}^{+\infty} H_{in-phase,k,j}(\omega + \frac{2\pi p}{T}) \quad (11.1)$$

$$FH_{quadrature,k,j}(\omega) = \sum_{p=-\infty}^{+\infty} H_{quadrature,k,j}(\omega + \frac{2\pi p}{T}) \quad (11.2)$$

Therefore, $I_{k,j}((m\text{-}n)T)$ and $Q_{k,j}((m\text{-}n)T)$ are proportional to the Fourier series coefficients of $FH_{\text{in-phase},k,j}(\omega)$ and $FH_{\text{quadrature},k,j}(\omega)$ respectively, which can be determined by $H_s(\omega)$ and $H_{D,j}(\omega + \omega_j)$ with Eqs. (3) and (11).

**Table 1. The Contributions to the Decoded $a'_{j,m}$ (the $m^{th}$ Sample of the $j^{th}$ Channel) in the Conventional System without $T$/2 Time Offset for the Quadrature Tributary***

| | the contribution of the $(m\text{-}1)^{th}$ symbol | the contribution of the $m^{th}$ symbol | the contribution of the $(m + 1)^{th}$ symbol |
|---|---|---|---|
| channel ($j$-2) | $-0.036a_{j\text{-}2,m\text{-}1}$ | $0.072a_{j\text{-}2,m}$ | $-0.036a_{j\text{-}2,m+1}$ |
| channel ($j$-1) | $-0.05b_{j\text{-}1,m\text{-}1}$ | $-0.1b_{j\text{-}1,m}$ | $-0.05b_{j\text{-}1,m+1}$ |
| channel $j$ | $0.056a_{j,m\text{-}1}$ | $a_{j,m}$ | $0.056a_{j,m+1}$ |
| channel ($j$ + 1) | $-0.05b_{j+1,m\text{-}1}$ | $-0.1b_{j+1,m}$ | $-0.05b_{j+1,m+1}$ |
| channel ($j$ + 2) | $-0.036a_{j+2,m\text{-}1}$ | $0.072a_{j+2,m}$ | $-0.036a_{j+2,m+1}$ |

*All terms are normalized by $I_{j,j}(0)$. $h_s(t)$ and $h_{D,j}(t)\exp(-i\omega_j t)$ are both raised-cosine shaped with the roll-off coefficient of 0.4.

**Table 2. The Contributions to the Decoded $a'_{j,m}$ (the $m^{th}$ Sample of the $j^{th}$ Channel) in Offset-QAM CoWDM***

| | the contribution of the $(m\text{-}1)^{th}$ symbol | the contribution of the $m^{th}$ symbol | the contribution of the $(m + 1)^{th}$ symbol |
|---|---|---|---|
| channel ($j$-2) | $-0.036a_{j\text{-}2,m\text{-}1}$ | $0.072a_{j\text{-}2,m}$ | $-0.036a_{j\text{-}2,m+1}$ |
| channel ($j$-1) | 0 | 0 | 0 |
| channel $j$ | $0.056a_{j,m\text{-}1}$ | $a_{j,m}$ | $0.056a_{j,m+1}$ |
| channel ($j$ + 1) | 0 | 0 | 0 |
| channel ($j$ + 2) | $-0.036a_{j+2,m\text{-}1}$ | $0.072a_{j+2,m}$ | $-0.036a_{j+2,m+1}$ |

*All terms are normalized by $I_{j,j}(0)$. $h_s(t)$ and $h_{D,j}(t)\exp(-i\omega_j t)$ are both raised-cosine shaped with the roll-off coefficient of 0.4.

#148015 - $15.00 USD Received 25 May 2011; revised 7 Jul 2011; accepted 8 Jul 2011; published 14 Jul 2011

Tables 1 and 2 compare the calculated signal level, ISI and crosstalk on the received $m^{th}$ sample of the in-phase tributary of the $j^{th}$ channel ($a'_{j,m}$ in Eq. (5.1)) for the conventional system and offset-QAM CoWDM respectively. The signal pulse shape before demultiplexing and the impulse response of the demultiplexing filter in both tables are raised cosine with the roll-off coefficient of 0.4. The phase difference between channels is $\pi/2$. Note that in the conventional system, the crosstalk level is only weakly dependent on this phase difference [13]. We can clearly see that offset-QAM CoWDM can eliminate the crosstalk from the adjacent channels ($j$-1) and ($j$ + 1), so would improve the performance when compared to the conventional system. It is also observed that in offset-QAM CoWDM, the crosstalk from channels ($j$-2) and ($j$ + 2) is still not fully eliminated due to the infinite spectral tails of raised-cosine signal pulse.

Tables 3 and 4 illustrate another example with $H_s(\omega)$ and $H_{D,j}(\omega + \omega_j)$ both being the square root of a raised-cosine function with the roll-off coefficient of 0.4. The phase difference between channels is $\pi/2$. In the conventional system (Table 3), the bandwidth-limited signal spectrum results in the crosstalk only arising from the adjacent channels ($j$-1) and ($j$ + 1). However, the crosstalk levels from not only the $m^{th}$ symbol but also the $(m\text{-}1)^{th}$ and $(m + 1)^{th}$ symbols of channels ($j$-1) and ($j$ + 1) are increased when compared to Table 1 because of the long pulse tails in the time domain. Therefore, the total crosstalk levels might not be reduced. In contrast, crosstalk and ISI free operation can be achieved when using offset-QAM CoWDM. It can be proved that in this case, the requirements (a)–(e) in subsection 2.1 are satisfied. In practice, this function can be readily achieved by using commercial components.

**Table 3. The Contributions to the Decoded $a'_{j,m}$ (the $m^{th}$ Sample of the $j^{th}$ Channel) in the Conventional System without $T/2$ Time Offset for the Quadrature Tributary***

| | the contribution of the $(m\text{-}1)^{th}$ symbol | the contribution of the $m^{th}$ symbol | the contribution of the $(m + 1)^{th}$ symbol |
|---|---|---|---|
| channel ($j$-2) | 0 | 0 | 0 |
| channel ($j$-1) | $0.109b_{j-1,m-1}$ | $-0.127b_{j-1,m}$ | $0.109b_{j-1,m+1}$ |
| channel $j$ | 0 | $a_{i,m}$ | 0 |
| channel ($j$ + 1) | $0.109b_{j+1,m-1}$ | $-0.127b_{j+1,m}$ | $0.109b_{j+1,m+1}$ |
| channel ($j$ + 2) | 0 | 0 | 0 |

*All terms are normalized by $I_{j,j}(0)$. $H_s(\omega)$ and $H_{D,j}(\omega + \omega_j)$ are both the square root of a raised-cosine function with the roll-off coefficient of 0.4.

**Table 4. The Contributions to the Decoded $a'_{j,m}$ (the $m^{th}$ Sample of the $j^{th}$ Channel) in Offset-QAM CoWDM***

| | the contribution of the $(m\text{-}1)^{th}$ symbol | the contribution of the $m^{th}$ symbol | the contribution of the $(m + 1)^{th}$ symbol |
|---|---|---|---|
| channel ($j$-2) | 0 | 0 | 0 |
| channel ($j$-1) | 0 | 0 | 0 |
| channel $j$ | 0 | $a_{i,m}$ | 0 |
| channel ($j$ + 1) | 0 | 0 | 0 |
| channel ($j$ + 2) | 0 | 0 | 0 |

*All terms are normalized by $I_{j,j}(0)$. $H_s(\omega)$ and $H_{D,j}(\omega + \omega_j)$ are both the square root of a raised-cosine function with the roll-off coefficient of 0.4.

## 3. Simulation Setup

In addition to the theoretical analysis, we numerically investigate the performance improvement enabled by the proposed system. Figure 3 shows the simulation setup, which was implemented using Matlab. A continuous wave (CW) light with 6kHz laser linewidth was fed into an optical comb generator to obtain five carriers with equal intensities and phases. The channel spacing was 25GHz, equal to the symbol rate per carrier. The signal data trains consisted of 25Gbit/s $2^{11}$-1 pseudo-random binary sequences (PRBS) repeated 5 times (10,235 bits). Different delays were applied to each tributary of the multi-level formats and also to each channel to ensure that their bit sequences were uncorrelated. These logic data trains were

#148015 - $15.00 USD Received 25 May 2011; revised 7 Jul 2011; accepted 8 Jul 2011; published 14 Jul 2011

used to generate multi-level electrical signals with 40 samples per symbol and raised-cosine pulse shape with the roll-off coefficient of 0.4. The quadrature signal was delayed by $T/2$ with respect to the in-phase signal (see the Inset of Fig. 1). These analogue electrical signal outputs were amplified and used for data modulation. The equivalent frequency response of the driving amplifier and the modulator's electronic interface was assumed to 3rd-order Gaussian or 5th-order Bessel shaped. The modulated optical signals were phase controlled by adding an additional phase $\phi_k = (k\text{-}1)\cdot\phi$, $k = 1\ldots5$ before they were combined. At the receiver, the noise of the optical preamplifier was modeled as additive white Gaussian noise. The launch power into the preamplifier was adjusted to control the optical signal-to-noise ratio (OSNR). An optical band-pass filter (OBPF) was not used because in a linear coherent receiver, any functionality of an OBPF could be performed by an electrical filter (EF). The signal and local oscillator were mixed by a 90° optical hybrid and detected by balanced detectors to extract the in-phase and quadrature tributaries. The powers of the local oscillator and the received signal were 10dBm and 3dBm respectively and their polarizations were controlled to be the same. The equivalent thermal noise spectral power density of the detectors was 18pA/Hz$^{1/2}$. After detection, the signals were electrically amplified and filtered by 3rd-order Gaussian-shaped EFs. The received analogue signals were sampled by analogue-to-digital converters (ADCs) with two samples per symbol and 8-bit physical resolution, unless otherwise stated. The sampled signals were fed into a finite impulse response (FIR) filter, which employed mean-square error criterion to update the FIR coefficients. Then the equalized signal was decoded to evaluate the bit error rate (BER) performance.

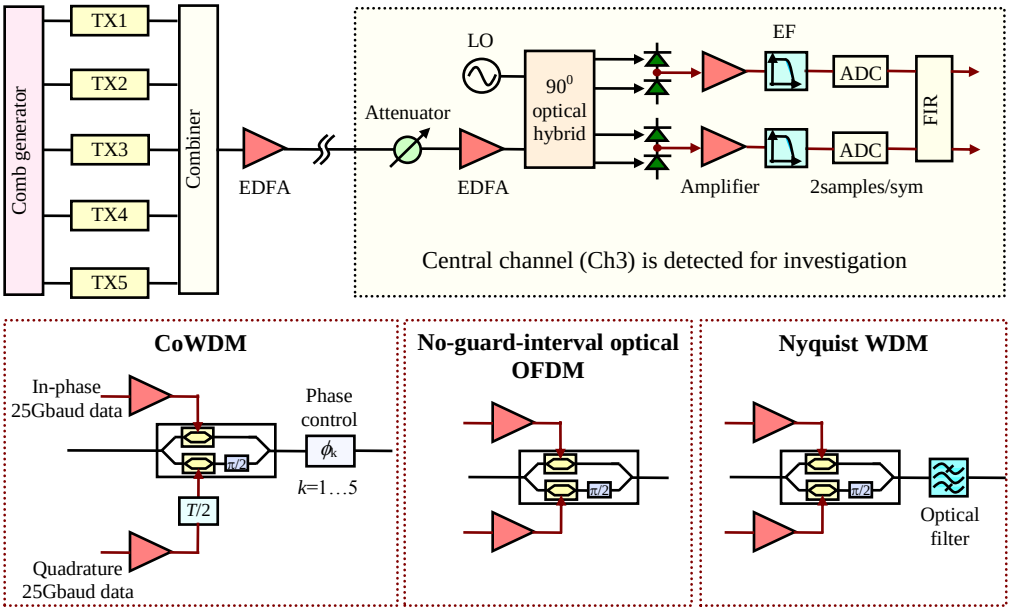


Fig. 3. Simulation setup for systems of offset-QAM CoWDM, no-guard-interval optical OFDM, and N-WDM, with 25Gsym/s per channel and 25GHz channel spacing.

For comparison, conventional no-guard-interval optical OFDM and Nyquist WDM were also simulated. In the former case, the simulation setup was similar to that of the offset-QAM CoWDM except that there was no $T/2$ time offset for the quadrature tributary. In the latter case, pre-filtering was used such that the output of the pre-filter had a raised-cosine shaped spectrum with the roll-off coefficient of 0.1 [5]. The –6dB bandwidth of the output of the pre-filter was 12.5GHz, unless otherwise stated. Note that because the performance of these two systems was only weakly dependent on the phase difference between channels [13], separate lasers with proper wavelength spacing instead of an optical comb generator could be used. All

#148015 - $15.00 USD Received 25 May 2011; revised 7 Jul 2011; accepted 8 Jul 2011; published 14 Jul 2011

simulations were iterated with different random number seeds to give a total of around 200,000 simulated bits. The performance was evaluated in terms of the required normalized OSNR to achieve a BER of $5 \times 10^{-4}$ for the central channel by direct error counting, where

$$Normalized \;\; OSNR = \frac{Total\ Signal\ Power}{5 \times Noise\ Power\ in\ 0.1nm} \tag{12}$$

## 4. Results

### *4.1 Comparison of Fundamental Performance Limit*

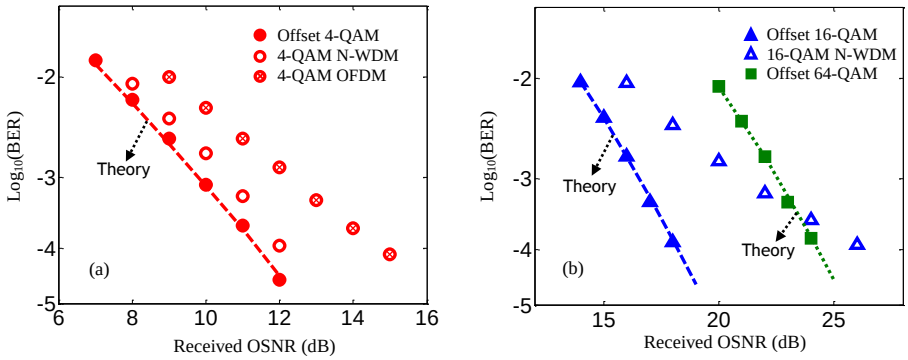


Fig. 4. (a). Performance versus the received OSNR for offset-QAM CoWDM (solid circles), Nyquist WDM (empty circles), and no-guard-interval optical OFDM (cross circles) using 4-QAM format. (b) Performance versus the received OSNR for CoWDM using offset 16- (solid triangles) and 64-QAM (solid squares), and for 16-QAM N-WDM (empty triangles). Dashed or dotted lines represent the theoretical limits. The phase difference between channels is $\pi/2$.

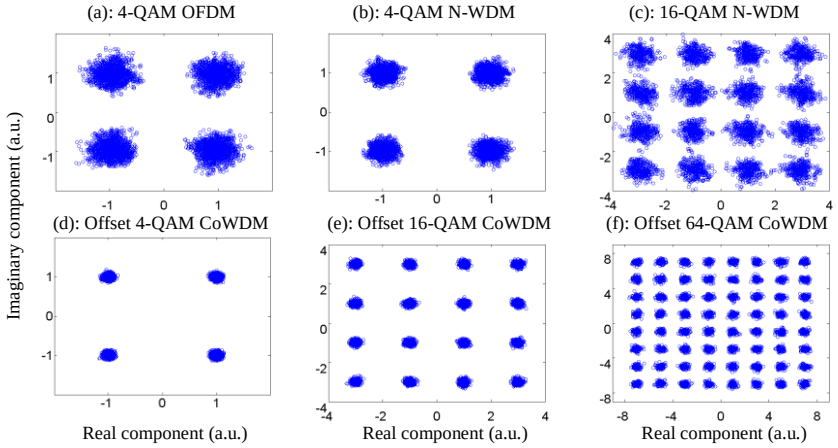


Fig. 5. Constellation diagrams of (a): 4-QAM no-guard-interval optical OFDM; (b): 4-QAM N-WDM; (c): 16-QAM N-WDM; (d): offset 4-QAM CoWDM; (e): offset 16-QAM CoWDM; (f): offset 64-QAM CoWDM. The system parameters are the same as Fig. 4.

Figure 4(a) and (b) show the simulated performance versus the received OSNR for offset-QAM CoWDM, no-guard-interval optical OFDM, and N-WDM under optimized transmitter and receiver bandwidths. The corresponding constellation diagrams are depicted in Fig. 5(a)–5(f). In Fig. 4 and 5, the equivalent response of the driving amplifier and the modulator's electronic interface was 3rd-order Gaussian shaped, which was found to result in better performance than a 5th-order Bessel shaped response. Note that in N-WDM, the signal

#148015 - $15.00 USD Received 25 May 2011; revised 7 Jul 2011; accepted 8 Jul 2011; published 14 Jul 2011

spectral profile from the output of the pre-filter was fixed regardless of this equivalent response. The memory length of the receiver FIR filter was 6 for offset-QAM CoWDM and no-guard-interval optical OFDM, and 12 for Nyquist WDM. The phase difference between channels was $\pi/2$. It can be seen from the figures that no-guard-interval optical OFDM exhibited the worst performance, and even with optimized transmitter and receiver bandwidths, this technique had around 3dB penalty at BER of $5 \times 10^{-4}$ for the 4-QAM format and could not support the 16-QAM format. On the other hand, Nyquist WDM used rectangular spectral profile and improved the performance by using optical pre-filtering. However, residual crosstalk still existed, which resulted in ~5dB penalty for 16-QAM at BER of $5 \times 10^{-4}$. In contrast, the presented system showed very clear constellation diagrams even for offset 64-QAM and the performance could approach the fundamental limits using practical devices with optimized bandwidths. This clearly illustrates the performance benefits of the proposed system, with the potential to achieve crosstalk and ISI free operation.

*4.2 Relaxed Transmitter Specifications*

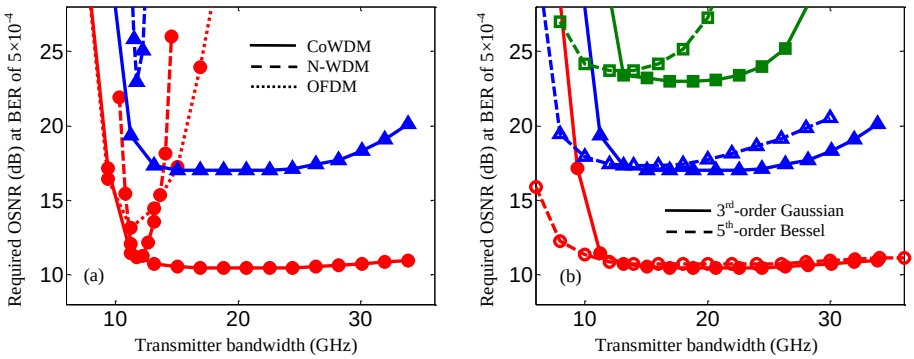


Fig. 6. (a) Required OSNR (dB) versus the transmitter bandwidth for CoWDM (solid), N-WDM (dashed), and no-guard-interval optical OFDM (dotted). Circles and triangles represent (offset) 4- and 16-QAM respectively (b) Required OSNR (dB) versus the transmitter bandwidth for offset 4- (circles), 16- (triangles), and 64-QAM (squares) CoWDM. The equivalent response of the driving amplifier and the modulator's electronic interface is 3rd-order Gaussian (solid) or 5th-order Bessel (dashed) shaped. For (a) and (b), the receiver EF bandwidth is optimized.

Figures 4 and 5 are based on the optimized system parameters. In practice, it would be essential to understand the performance sensitivity to the specifications of system components. Figure 6(a) shows the performance versus the transmitter bandwidth under optimized receiver EF bandwidth, where the transmitter bandwidth is defined as the equivalent bandwidth of the driving amplifier and the modulator's electronic interface in offset-QAM CoWDM and no-guard-interval optical OFDM, but in N-WDM, represents the bandwidth of the output from the pre-filter. The memory length of the receiver FIR filter was 6 for offset-QAM CoWDM and no-guard-interval optical OFDM, and 12 for N-WDM. The phase difference between channels was $\pi/2$. The figure clearly shows that the conventional systems, in particular N-WDM, were sensitive to the transmitter bandwidth, because careful design was required to balance the ISI and the crosstalk from the adjacent channels 2 and 4. In contrast, offset-QAM CoWDM could completely eliminate the crosstalk from channels 2 and 4, provided that the signal pulse was an even function (true for most practical signal pulse) and matched filter was used at the receiver (obtained by the receiver FIR filter). The transmitter bandwidth had only to be limited to sufficiently suppress the crosstalk from channels 1 and 5. Consequently, the specifications of the transmitter were greatly relaxed, with optimal performance for a wide bandwidth range from 12GHz to 30GHz. On the other hand, offset 16-QAM was more sensitive to the residual ISI and crosstalk, so exhibited higher

#148015 - $15.00 USD Received 25 May 2011; revised 7 Jul 2011; accepted 8 Jul 2011; published 14 Jul 2011

penalty when the transmitter bandwidth was smaller than 12GHz or larger than 30GHz when compared to offset 4-QAM.

Figure 6(b) shows the performance versus the transmitter bandwidth for two types of transmitter responses in offset-QAM CoWDM. It is found that 3rd-order Gaussian shaped response exhibited slightly better optimal performance and could support a larger transmitter bandwidth when compared to the 5th-order Bessel shaped response. This is because the sharp roll-off of the 3rd-order Gaussian response would suppress the crosstalk from channels 1 and 5 more effectively for a larger transmitter bandwidth, resulting in better performance especially for higher-level formats. However, this sharp roll-off also introduced more ISI and degraded the performance when the transmitter bandwidth was small.

*4.3 Relaxed Receiver Specifications*

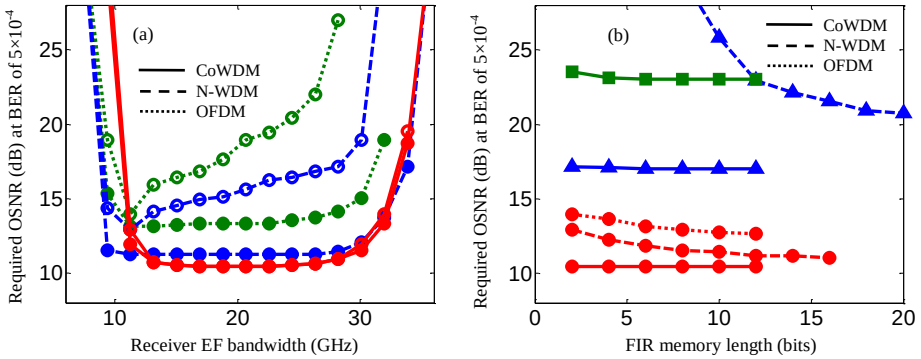


Fig. 7. (a) Required OSNR (dB) versus the receiver EF bandwidth for offset 4-QAM CoWDM (solid lines), 4-QAM N-WDM (dashed lines), and 4-QAM no-guard-interval optical OFDM (dotted lines). Solid symbols represent a FIR memory length of 6 for CoWDM and OFDM, or 12 for N-WDM. Empty symbols represent a FIR memory length of 2 for CoWDM, OFDM, and N-WDM. (b) Required OSNR (dB) versus the memory length of the receiver FIR filter. Circles, triangles, and squares represent (offset) 4-, 16-, and 64-QAM respectively. For (a) and (b), the transmitter bandwidth is optimized and the phase difference between channels is $\pi/2$.

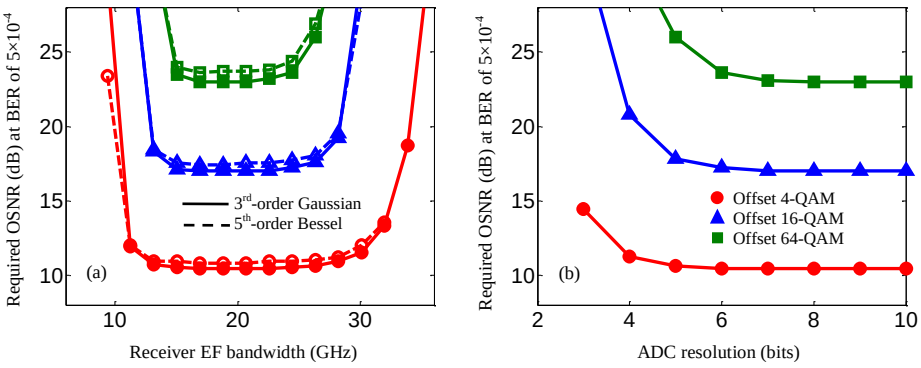


Fig. 8. (a) Required OSNR (dB) versus receiver filter bandwidth for offset 4- (circles), 16- (triangles), and 64-QAM (squares) CoWDM when the equivalent response of the driving amplifier and the modulator's electronic interface is 3rd-order Gaussian (solid) and 5th-order Bessel (dashed). The transmitter bandwidth is optimized. (b) Required OSNR (dB) versus the ADC resolution for offset 4- (circles), 16- (triangles), and 64-QAM (squares) CoWDM under optimized transmitter and receiver bandwidths. In (a) and (b), the receiver FIR filter memory length is 6 and the phase difference between channels is $\pi/2$.

#148015 - $15.00 USD Received 25 May 2011; revised 7 Jul 2011; accepted 8 Jul 2011; published 14 Jul 2011

In addition to the relaxed transmitter specifications, the presented system also reduces the requirements for the receiver specifications under optimized transmitter bandwidth. Figure 7(a) illustrates the performance as a function of the receiver EF bandwidth for CoWDM, N-WDM and no-guard-interval optical OFDM with varied memory length of the receiver FIR filter when the response of the driving amplifier and the modulator was 3rd-order Gaussian shaped. Note that the signal spectrum of the output from the pre-filter in N-WDM was fixed regardless of this response. The phase difference between channels was assumed to be $\pi/2$. It is further confirmed that under optimized transmitter and receiver bandwidths, offset-QAM CoWDM exhibited better performance than the no-guard-interval optical OFDM and N-WDM. In addition, the tolerance range of the receiver EF bandwidth was almost unchanged even when the memory length of the receiver FIR filter was reduced to 2. In contrast, in the no-guard-interval optical OFDM and N-WDM, when the receiver EF bandwidth was larger than 12GHz, the balance of ISI and crosstalk could not be well performed by using a memory length of 2. Consequently, the bandwidth tolerance range was reduced. The conclusion was further confirmed in Fig. 7(b). It can be clearly seen that CoWDM was insensitive to the memory length even for offset 64-QAM. On the other hand, the no-guard-interval optical OFDM and N-WDM required a larger memory length to obtain the optimal performance, especially for higher-level modulation formats. In the 16-QAM N-WDM, the optimal performance could not be achieved even for a memory length as large as 20 bits.

More investigations on the required receiver specifications for offset-QAM CoWDM are shown in Fig. 8(a), where the required OSNR versus the receiver EF bandwidth using varied modulation formats and transmitter responses are depicted. Similar to Fig. 6(b), 3rd-order Gaussian shaped response for the driving amplifier and the modulator's electronic interface resulted in better performance. The bandwidth tolerance range was reduced when the format level increased due to the increased sensitivity to residual ISI and crosstalk.

In Fig. 4–8(a), the ADC resolution was assumed to be 8 bits. It would be important in practice to understand the performance variations associated with the ADC resolutions, as shown in Fig. 8(b). In the figure, the transmitter and receiver bandwidths were optimized and the memory length of the FIR filter was 6. It is observed that the required ADC resolution depended on the format level. However, less than 1dB penalty could be ensured by using 6-bit resolution even for offset 64-QAM CoWDM. This resolution could be readily achieved by the state-of-the-art commercial ADC products.

*4.4 Performance Sensitivity to Phase Difference between Channels*

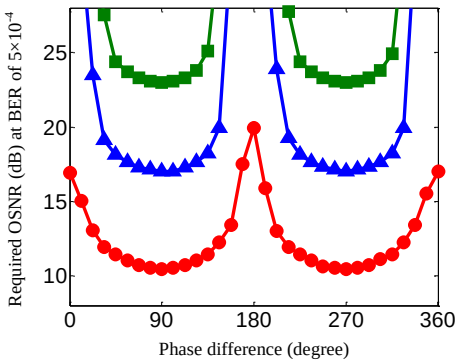


Fig. 9. Performance as a function of phase difference between channels for 3rd-order Gaussian shaped transmitter and receiver EF with optimized bandwidths. Circles, triangles, and squares represent offset 4-, 16-, and 64-QAM respectively.

It was theoretically proved in Section 2 that one of necessary conditions to achieve crosstalk free operation was the control of the phase difference between channels. This conclusion is

#148015 - $15.00 USD Received 25 May 2011; revised 7 Jul 2011; accepted 8 Jul 2011; published 14 Jul 2011

numerically confirmed in Fig. 9, which shows the performance versus the phase difference between channels under optimized transmitter and receiver filter bandwidths. The memory length of the receiver FIR filter was 6. The figure shows that the performance of the proposed offset-QAM system depended on the phase difference between channels such that phase control at the transmitter, i.e. CoWDM, was needed. In this aspect, the implementation complexity was increased when compared to the no-guard-interval optical OFDM. It is also shown that the optimal performance was obtained when the phase difference was $\pi/2$ or $3\pi/2$. At 1dB OSNR penalty, the phase tolerance range was around ± 45°, ± 40°, ± 35° for offset 4-, 16-, and 64-QAM, respectively.

## 5. Conclusions

We have proposed and investigated a CoWDM system using offset 4-, 16-, and 64-QAM to significantly improve the performance and relax the device specifications. We have theoretically derived the condition for crosstalk free operation for the presented system and found that by offsetting the two quadratures by half symbol period in time, the crosstalk and ISI can be eliminated even using practical signal spectral profiles. Based on the implications of the analysis, we have numerically compared this system with recently reported no-guard-interval optical coherent OFDM and Nyquist WDM, and shown that the presented system significantly relaxes the specifications of the system components and enhances the spectral efficiency by enabling the use of higher-level modulation formats, with the achieved performance approaching the theoretical limits using practical devices.

## Acknowledgments

This work was supported by Science Foundation Ireland under grant number 06/IN/I969.

#148015 - $15.00 USD Received 25 May 2011; revised 7 Jul 2011; accepted 8 Jul 2011; published 14 Jul 2011